DEGRADATION OF AGROCHEMICALS IN WASTEWATERS BY THE PHOTO-FENTON PROCESS: EXPERIMENTAL STUDY USING UV MERCURY VAPOR LAMPS AND SOLAR IRRADIATION

Antonio C.S.C. Teixeira[1], Giselle Stollar, Roberto Guardani, Cláudio A.O. Nascimento
University of São Paulo – Chemical Engineering Department
Av. Prof. Luciano Gualberto, tr. 3, 380 - 05508-900 - São Paulo – SP – Brazil – Fax: +55-11-3813-2380
[1] E-mail: acscteix@usp.br

Key Words: photo-Fenton, agrochemicals, pesticides; wastewater

Introduction

Pesticides can be present in wastewater from industry and farm work operations (rinse water from spray equipment and empty pesticide containers, post-harvest washing of fruits and vegetables, etc.).[1] The inadequate management of these toxic recalcitrant residues can cause contamination of the soil and of subterranean and surface water sources. Social and legal demands for environmental safety require these impacts be minimized.

In general, wastewater remediation by conventional treatments (flocculation, adsorption, incineration, etc.), while often efficient, often merely transfers pollutants from one phase to another.[2] Also, the presence of non-biodegradable substances precludes the use of conventional activated-sludge systems. These demands have fueled the development of more effective and economically viable methods for pollution control and prevention.

Several photochemical advanced oxidation processes (AOPs) are known that can rather unselectively oxidize a wide range of organic pollutants with a diversity of chemical structures and functional groups.[2-4] Under favorable conditions, the total decomposition of the organic constituents of the pollutant to carbon dioxide and water, plus inorganic salts of all heteroatoms other than oxygen, is achieved.[5] In the AOPs carried out in homogeneous solution, the absorption of light triggers photochemical and/or chemical reactions that produce hydroxyl radicals ($HO^{\bullet}$), which react with the majority of organic substances with low selectivity and at rates often approaching the diffusion-controlled limit.[6]

Among AOPs, the photo-Fenton reaction is considered most promising for the remediation of wastewater containing a variety of toxic non-biodegradable organic compounds.[7] In the Fenton reaction, Fe(II) is oxidized to Fe(III), and H_2O_2 is reduced to the hydroxide ion and the hydroxyl radical:

$$Fe(II)+H_2O_2 \longrightarrow Fe(III)+HO^{\bullet}+OH^{-} \qquad (1)$$

In the absence of light, Fe(III) is reduced back to Fe(II) by hydrogen peroxide:

$$Fe(III)+H_2O_2+H_2O \longrightarrow Fe(II)+H_3O^{+}+HO_2^{\bullet -} \qquad (2)$$

Reaction 2 is much slower than reaction 1, and ultimately determines the overall process rate. For the degradation of organic molecules, the optimum pH for the Fenton reaction is typically in the range 3-4, and the optimum mass ratio $Fe(II)/H_2O_2$ is 1.5.[8] A more detailed description of these reactions, considering hydrated iron-H_2O_2 complexes, including rate constants and redox potentials is found in literature.[9]

Irradiation of Fenton systems with UV-visible irradiation strongly accelerates both Fenton and Fenton-like (H_2O_2/Fe(III)) reactions, improving degradation rates.[7] The optimum pH range is 2-4, in which the predominant Fe(III) species in aqueous solution is $Fe(OH)^{2+}$, which absorbs out to 410 nm, undergoing a relatively efficient internal light-induced redox reaction, yielding hydroxyl radicals and regenerating Fe(II) (reaction 3):[10]

$$Fe(OH)^{2+} \xrightarrow{h\nu} Fe(II)+HO^{\bullet} \qquad (3)$$

Also, photochemical reactions of Fe(III)-L (L=organic intermediates, specially acids) are reported. These species exhibit strong ligand-to-metal charge absorption bands in the near-UV and visible region of the spectrum (reaction 4):

$$Fe(III)\text{-}L \xrightarrow{h\nu} [Fe(III)\text{-}L]^{*} \xrightarrow{h\nu} Fe(II)+L^{\bullet} \qquad (4)$$

One of the common drawbacks of photochemical processes is the great demand of electrical energy for UV lamps.[7] This can easily represent 60% of the total operating expense of a lamp-based photochemical reactor. A very interesting alternative is the use of solar light, which looks extremely attractive at sites with annual global insolation of 1700 kWh m^{-2} or higher.[2] The solar radiation incident on the earth's surface is split up into the direct-beam radiation and the diffuse radiation.[11] Direct radiation is the solar radiation that reaches the surface without being scattered or

absorbed in the atmosphere. The diffuse component refers to scattered radiation. Comprehensive articles have been published for the last years concerning ongoing R&D directed towards solar photocatalytic reactors.[12]

Some papers have appeared in the literature describing the use of the photo-Fenton process for the degradation of waterborne pesticides. The degradation of triazine herbicides,[1] methyl-parathion,[3] fenuron[13], and diuron[1] are known examples. In this work, the variables involved in the photo-Fenton reaction, namely Fe(II) and H_2O_2 concentrations, radiation source, and pesticide chemical structure, were investigated in detail.

Methodology

A schematic view of the bench-scale photochemical reactor used in this work is shown in Fig. 1. The equipment consisted of an annular photochemical reactor (Ace Glass, model 7863-20) with a net volume of 0.85 L, connected to a 1-L jacketed glass reservoir.

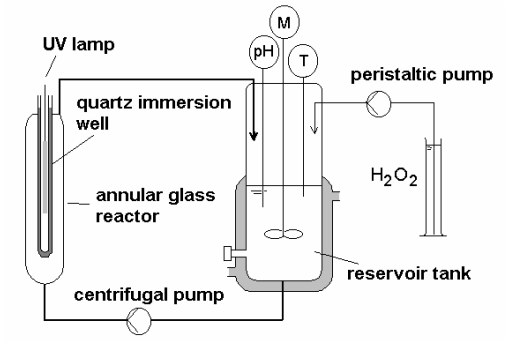

Figure 1 - Schematic view of the bench-scale photochemical reactor. M, rotating impeller connected to an agitator device. T, temperature sensor connected to a digital indicator. pH, electrode connected to a digital pH meter.

Two liters of the pesticide solution was circulated through the reactor and the tank at 0.025 L s^{-1}, and its temperature was controlled by means of a thermo-regulated bath. The light source was a medium pressure mercury vapor lamp (Philips, model HPLN) placed inside a quartz-well (cutting-off radiation of wavelength shorter than 280 nm). Ferrioxalate actinometry measurements[9] indicated average polychromatic photon fluxes of 2.2×10^{19} and 4.6×10^{19} photons s^{-1} for 125 and 400-W lamps, respectively.

A schematic view of the concentrating parabolic-trough reactor (PTR) used in the solar experiments is shown in Fig. 2. The apparatus consisted of nine flow-through borosilicate glass tubes in series, connected to a 10-L reservoir. 5 L of pesticide aqueous solution was treated in each batch, circulated at 30 L min^{-1} by means of a centrifugal pump. Each tube was positioned at the line-focus of a parabolic trough collector of 0.26 m^2 reflecting surface. The PTR was mounted on a fixed platform inclined 23º (from ground) and facing North, according to the latitude (23º32.0'S) and longitude (46º37.0'W) of São Paulo (Brazil).

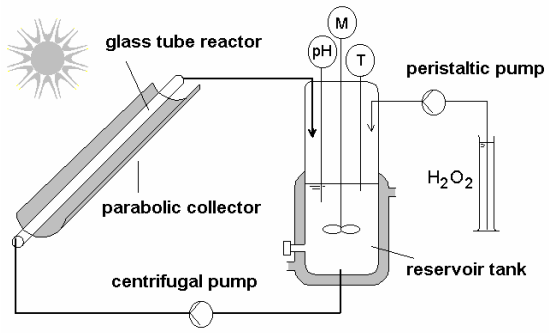

Figure 2 - Schematic view of the concentrating parabolic-trough reactor (PTR), showing one tube. M, rotating impeller connected to an agitator device. T, temperature sensor connected to a digital indicator. pH, electrode connected to a digital pH meter.

The experimental procedure was the same in all runs. The pesticide aqueous solution, prepared from commercial agrochemical formulations or from the active compounds, was firstly introduced into the reactor. pH was adjusted at 3.0 by the addition of H_2SO_4, and then continuously monitored. Weighed amount of solid $FeSO_4.7H_2O$ (>98%, Sigma Aldrich) was added, and the system was exposed to light. The H_2O_2 solution, prepared using an analytical grade stock-solution (30% w/w in water, Merck), was introduced at a controlled flow rate (13.3 μL s^{-1}), by means of a peristaltic pump (Ismatec-IPC). In the following sections, $[H_2O_2]$ refer to the hydrogen peroxide concentration of the feed solution, and [Fe(II)] to the iron concentration of the aqueous solution in the reactor.

Ten-milliliter samples were taken from the reservoir at specified times for the characterization of pollutant degradation. The chemical oxygen demand (COD) of each sample was measured by the closed-reflux colorimetric method.[14] The concentration of dissolved organic carbon (DOC) was measured using the Shimadzu 5000A equipment. A quenching solution containing KI, Na_2SO_3 and NAOH (0.1 mol L^{-1} each) was added to the samples in the proportion 5:2 v/v (sample:solution) in order to decompose residual H_2O_2 and precipitate iron species. All samples were filtered through a 0.22-μm membrane before DOC analysis. The biochemical oxygen demand (BOD_5) of the final treated solution was measured by the respirometric method[14] using the Oxitop IS 12 manometric respirometer (WTW).

The Laboratory of Micrometeorology (Astronomical and Geophysical Institute, University of São Paulo) provided solar radiation data. Global radiation was measured every five minutes with a pyranometer (Eppley, model PBW) in the range 285 to 2800 nm. The diffuse component was measured by means of a pyranometer (Eppley, model PSP) with a shading ring to eliminate direct radiation. Fig. 3 shows a typical solar irradiance profile, and the corresponding accumulated radiant energy. Ferrioxalate actinometry indicated an average polychromatic photon flux equal to 1.9×10^{21} photons s^{-1}. All solar experiments were carried out within a few weeks, so that seasonal effects were not important.

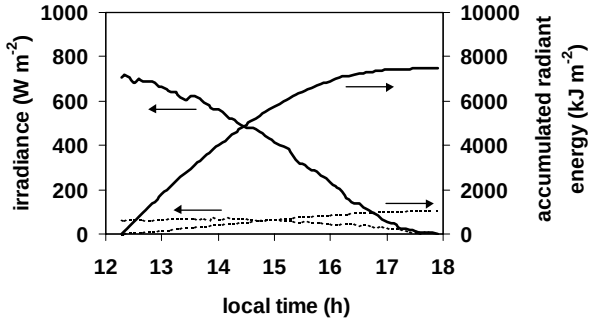

Figure 3 - Direct and diffuse (broken lines) radiation measurements (left ordinate axis) and corresponding accumulated radiant energy (right ordinate axis).

Results and Discussion

The photo-Fenton degradation of three agrochemicals was estudied: tebuconazole (fungicide), methamidophos (insecticide/acaricide), and clomazone (herbicide).

1. *experiments with tebuconazole*

Aqueous solutions (1 g L^{-1}) of tebuconazole ((RS)-1-*p*-chlorophenyl-4,4-dimethyl-3-(1H-1,2,4-triazol-1-ylmethyl)pentan-3-ol, Fig. 4), prepared with the formulation Folicur® PE (wettable powder, 25% w/v in active compound, Bayer CropScience), were used. These solutions had COD_0=224±27 mg L^{-1}; DOC_0=70±5 mg L^{-1}; BOD_5=187 mg L^{-1}. The results of the experiments are shown in Figs. 5 to 8.

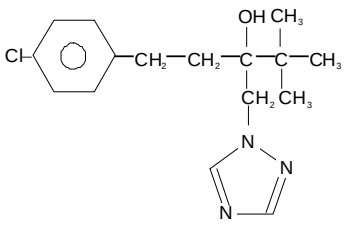

Figure 4 - Molecular structure of tebuconazole.

The photo-Fenton reaction (Fig. 5, experiment P8-L) showed a rapid removal of DOC (89%) and COD (86%). The increase in inorganic carbon concentration (3 to 18 mg L^{-1}) and the variation of pH (3 to 2.62, associated with the formation of organic acids) suggested the mineralization of tebuconazole and inert compounds. The dark Fenton process (experiment P13-L), on the other hand, showed a DOC removal of only 11%. In this case, the generation of $HO^{\bullet}$ radicals slowed down after reaction 1, and the addition of relatively large amounts of iron would be required in order to degrade the pollutant.[7,8]

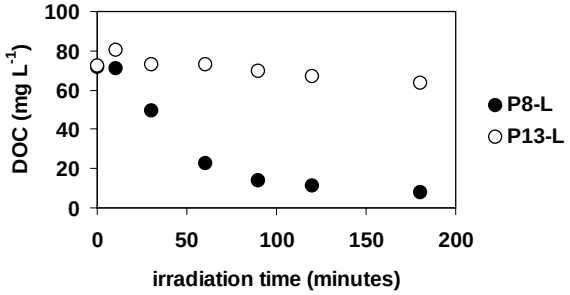

Figure 5 - Results of the experiments carried out with tebuconazole at 30°C, 400-W lamp. P8-L (photo-Fenton; $[H_2O_2]$=0.5 mol L^{-1}; [Fe(II)]=0.0005 mol L^{-1}); P13-L (Fenton; $[H_2O_2]$=0.5 mol L^{-1}; [Fe(II)]=0.0005 mol L^{-1}).

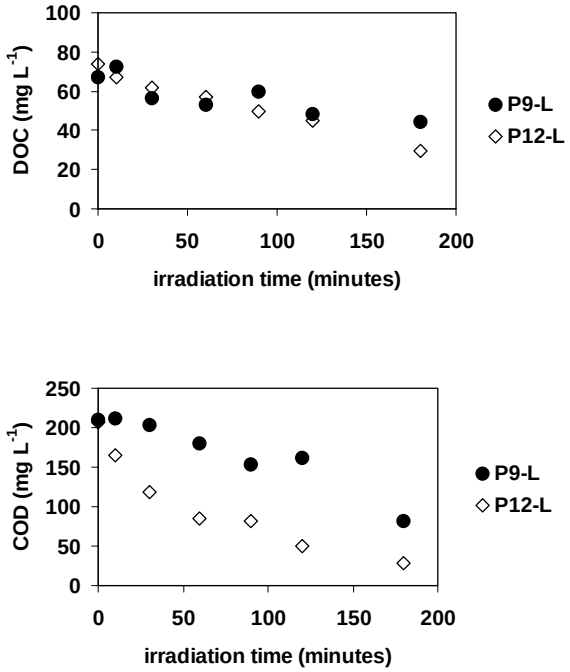

Figure 6 - Results of the photo-Fenton experiments carried out with tebuconazole, 400-W lamp. P9-L (30°C; $[H_2O_2]$=0.05 mol L^{-1}; [Fe(II)]=0.0005 mol L^{-1}); P12-L (50°C; $[H_2O_2]$=0.05 mol L^{-1}; [Fe(II)]=0.0005 mol L^{-1}).

Therefore, irradiation of the Fenton system not only regenerated Fe(II), the crucial catalytic species in the Fenton reaction (reactions 3 and 4), but also produced an additional $HO^{\bullet}$ radical, the species responsible for oxidative chain reactions. Moreover, since Fe(II) was regenerated by light, the photo-Fenton process consumed less H_2O_2 and required only catalytic amounts of Fe(II).

Fig. 6 shows that DOC-time curves were virtually the same at 30 and 50°C (experiments P9-L and P12-L). In experiment P12-L, the concentration of organic compounds that could be oxidized at any time should be smaller, while the carbon balance in both experiments was rather similar. In spite of the fact that reactions 3 and 4 are less sensitive to temperature,[6,7,10] this could suggest different reaction pathways at each temperature.

Fig. 7 indicates that increasing $[H_2O_2]$ in the range 0.01-0.1 mol L^{-1} had not a significant effect. For $[H_2O_2]$=0.5 mol L^{-1} (experiment P8-L), DOC and COD removals of 68 and 73%, respectively, were obtained in the first 60 minutes. DOC and COD percent removals after 180 minutes were about 90%, associated with a rapid variation in pH values from 3.00 to 2.62, measured after 30 minutes.

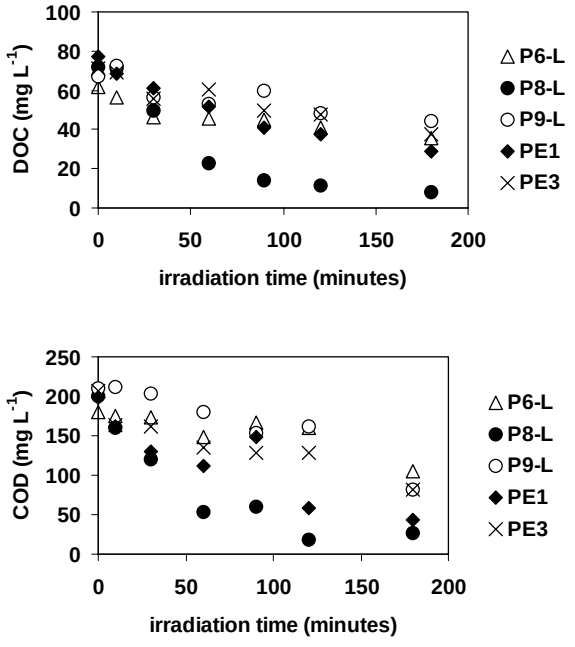

Figure 7 - Results of the photo-Fenton experiments carried out with tebuconazole at 30°C, 400-W lamp. P6-L ($[H_2O_2]$=0.05 mol L^{-1}; Fe(II)]=0.0028 mol L^{-1}); P8-L ($[H_2O_2]$=0.5 mol L^{-1}; Fe(II)]=0.0005 mol L^{-1}); P9-L ($[H_2O_2]$=0.05 mol L^{-1}; Fe(II)]=0.0005 mol L^{-1}); PE1 ($[H_2O_2]$=0.1 mol L^{-1}; Fe(II)]=0.00055 mol L^{-1}); PE3 ($[H_2O_2]$=0.01 mol L^{-1}; Fe(II)]=0.00055 mol L^{-1}).

Fig 7. also shows that a five-fold increase in [Fe(II)] did not seem to have a significant effect on DOC and COD-time-evolution. This behavior could be attributed to the photocatalytic effect.[7]

BOD_5 was determined for samples taken at t=0 and t=180 minutes for a photo-Fenton experiment carried at 30°C, $[H_2O_2]$=0.055 mol L^{-1}, and [Fe(II)]=0.00055 mol L^{-1}. Fig. 8 shows a final COD removal of 66%, along with an almost five-fold increase in BOD_5. The BOD_5/COD ratio varied from 2.7 to 36%. The increased biodegradability was of great importance, in view of the use of the photo-Fenton reaction as a preliminary step prior to a conventional activated-sludge biological treatment.

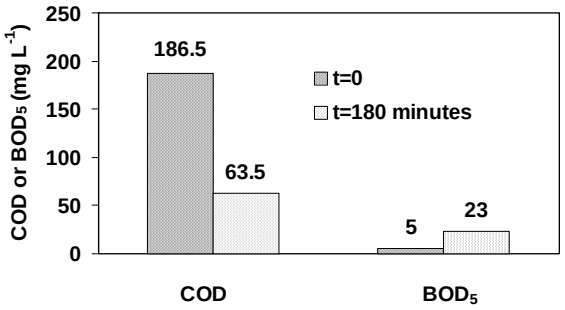

Figure 8 – Results of the photo-Fenton experiment carried out with tebuconazole at 30°C, $[H_2O_2]$=0.055 mol L^{-1}; [Fe(II)]=0.00055 mol L^{-1}, 400-W lamp.

2. *experiments with methamidophos*

The experiments with methamidophos ((RS)-O,S-dimethyl phosphoramidothioate, Fig. 9), were carried out with an aqueous solution (1 mL L^{-1}) of the formulation Tamaron® BR (concentrated liquid emulsion, 60% w/v in active compound, Bayer CropScience), which had COD_0=864±12 mg L^{-1}; DOC_0=245±8 mg L^{-1}; and BOD_5=5 mg L^{-1}. The results are presented in Fig. 10.

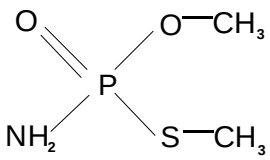

Figure 9 - Molecular structure of methamidophos.

Fig. 10 shows a slow decrease of DOC values with time for experiments TM1 and TM2 (final removals of 6 and 18%, respectively). A huge increase in $[H_2O_2]$ together with an increase in [Fe(II)] were needed to obtain the behavior shown after 60 minutes in experiment TM3, with 82% carbon removal after 180 minutes. These results also suggest the generation of stable degradation products without a substantial variation in DOC

concentration, which could be mainly acids, since pH varied in the ranges 3.03-2.47 (TM1), and 3.04-2.01 (TM2). In experiment TM3, pH remained virtually constant, due to the excess of H_2O_2, and faster pollutant mineralization.

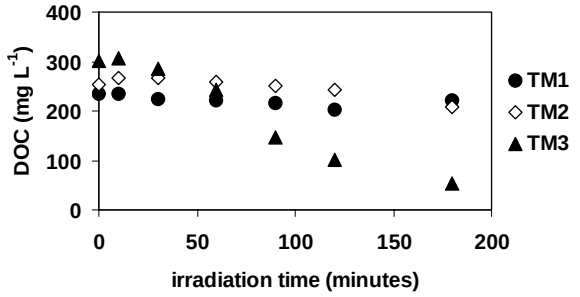

Figure 10 - Results of the photo-Fenton experiments carried out with methamidophos at 30°C, 400-W lamp. TM1 ([H_2O_2]=0.055 mol L^{-1}; [Fe(II)]=0.00055 mol L^{-1}); TM2 ([H_2O_2]=0.55 mol L^{-1}; [Fe(II)]=0.00055 mol L^{-1}); TM3 ([H_2O_2]=8 mol L^{-1}; [Fe(II)]=0.001 mol L^{-1}).

The comparison of COD results in Figs. 7 and 10 suggest that the principal mechanisms of reaction of hydroxyl radicals with organic compounds[9] seemed to be less operative in the case of methamidophos, owing to its recalcitrance. In fact, a small increase in [H_2O_2] had a more pronounced effect on tebuconazole degradation.

3. *experiments with clomazone*

In the case of clomazone (2-(2-chlorobenzyl)-4,4-dimethyl-1,2-oxazolidin-3-one, Fig. 11), aqueous solutions (0.185 g L^{-1}) of the active compound (91% w/v, Clariant) were used. These solutions had COD_0=271±35 mg L^{-1} and DOC_0=97±10 mg L^{-1}. A standard 24-h toxicity test with *Artemia* sp nauplii[15] resulted in CL_{50}=84 mg L^{-1}.

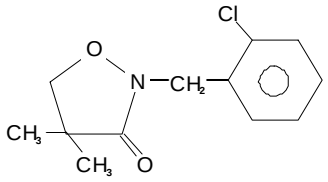

Figure 11 - Molecular structure of clomazone.

Experiments were carried out according to a Doehlert uniform experimental design,[16] in which the effects of the molar ratio H_2O_2:C and [Fe(II)] were studied at a constant photon flux (2.2×10^{19} photons s^{-1}, 125-W lamp). The experimental points can be represented as the apexes and the center of a hexagon (Fig. 12).

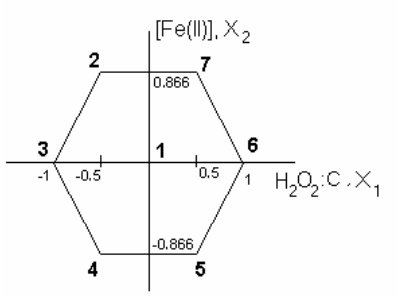

Figure 12 - Graphical representation of the Doehlert uniform array. Variables X_1 and X_2 are normalized. The experiment numbers are indicated near the apexes and the center of the hexagon.

Figs. 13 to 15 compare the results of the experiments in which [Fe(II)] was held constant at different levels. At [Fe(II)]=0.0001 mol L^{-1} (experiments CLZ-L4 and CLZ-L5, Fig. 13), the irradiation time, in minutes, required to achieve a DOC removal of 50% relative to the initial DOC (t_{50}) varied from 38 to 21 minutes when H_2O_2:C varied from 1.625 to 3.875, respectively. DOC removals after 180 minutes were about 88%. COD-time curves behaved similarly. In experiment CLZ-L5, pH decreased from 3.05 to 2.44.

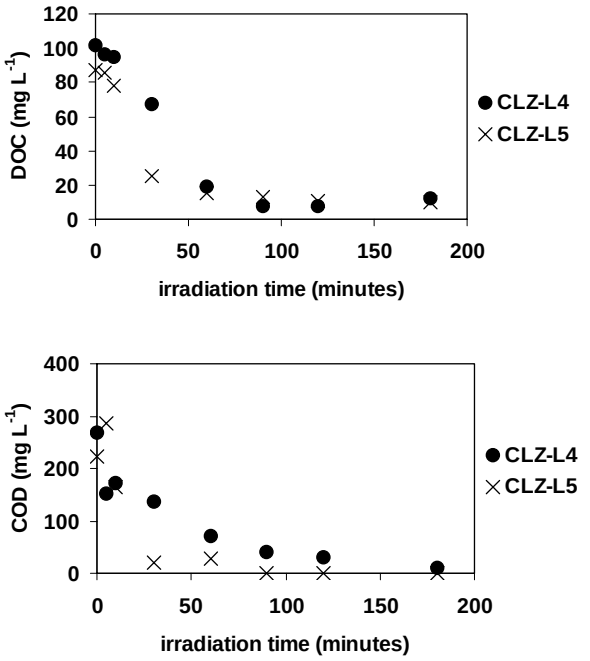

Figure 13 - Results of the photo-Fenton experiments carried out with clomazone at 30°C and [Fe(II)]=0.0001 mol L^{-1}, 125-W lamp. CLZ-L4 (H_2O_2:C=1.625); CLZ-L5 (H_2O_2:C=3.875).

Fig. 14 ([Fe(II)]=0.00055 mol L^{-1}) shows that a 5.5-fold increase in peroxide concentration enabled fast pesticide degradation. t_{50} varied from 87 to 19 and 8 minutes when H_2O_2:C varied from 0.5 to 2.75 and 5 (experiments CLZ-L3, CLZ-L1, and CLZ-L6,

respectively); the corresponding DOC removals after 180 minutes were 66, 88, and 88%, respectively.

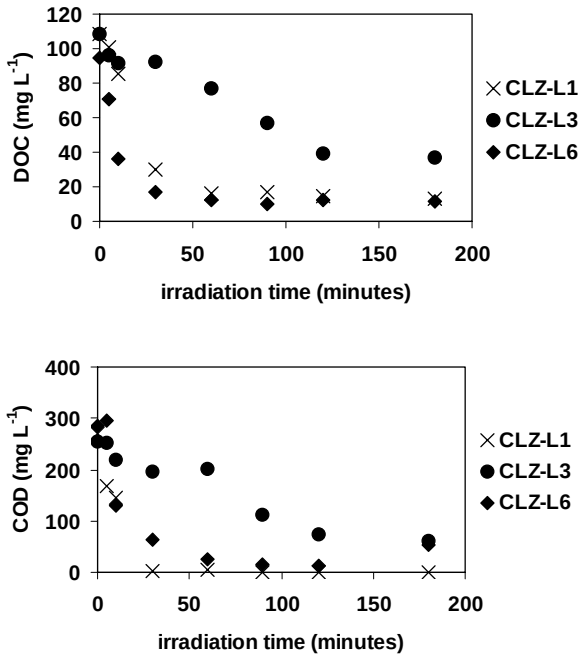

Figure 14 - Results of the photo-Fenton experiments carried out with clomazone at 30°C and [Fe(II)]=0.00055 mol L^{-1}, 125-W lamp. CLZ-L1 (H_2O_2:C=2.75); CLZ-L3 (H_2O_2:C=0.5); CLZ-L6 (H_2O_2:C=5).

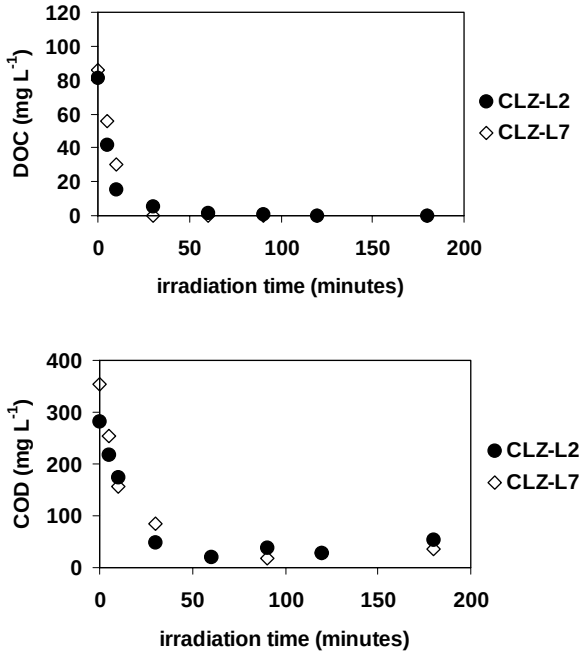

Figure 15 - Results of the photo-Fenton experiments carried out with clomazone at 30°C and [Fe(II)]=0.001 mol L^{-1}, 125-W lamp. CLZ-L2 (H_2O_2:C=1.625); CLZ-L7 (H_2O_2:C=3.875).

At the maximum Fe(II) concentration, Fig. 15 shows no remarkable modification of DOC and COD-time curves was observed when H_2O_2:C varied from 1.625 to 3.875 (experiments CLZ-L2 and CLZ-L7, respectively). Total mineralization of the pesticide was achieved in the first 30 minutes in both cases. The photo-Fenton degradation of clomazone should be less susceptible to peroxide concentration at high [Fe(II)] taking into account the importance of the thermal Fenton reactions.

Figs. 16 and 17 compare the results of the experiments in which H_2O_2:C was held constant at H_2O_2:C=1.625. The increase in the Fe(II) concentration from 0.0001 to 0.001 mol L^{-1} led to a decrease in t_{50} from 38 to 6 minutes, and to an increase in DOC removal after 180 minutes of irradiation from 88 to 100% (experiments CLZ-L4 and CLZ-L2, respectively).

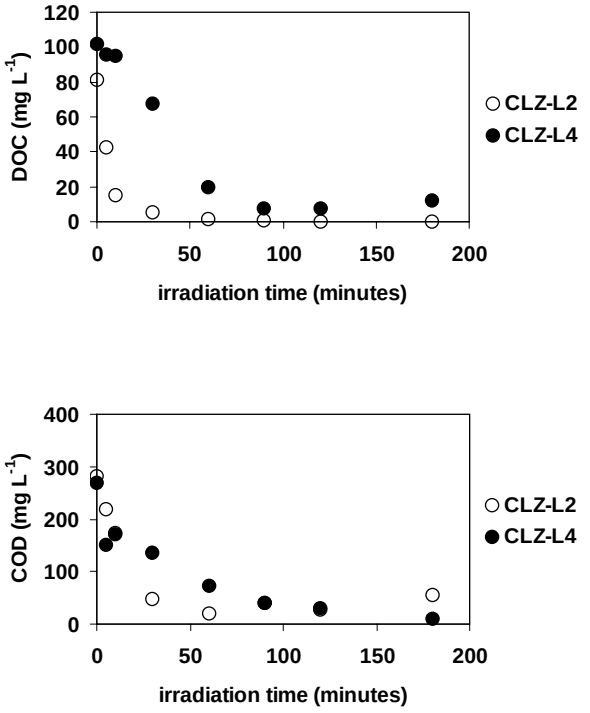

Figure 16 - Results of the photo-Fenton experiments carried out with clomazone at 30°C and H_2O_2:C=1.625, 125-W lamp. CLZ-L2 ([Fe(II)]=0.001 mol L^{-1}); CLZ-L4 ([Fe(II)]=0.0001 mol L^{-1}).

A similar but less remarkable behavior was obtained at H_2O_2:C=3.875 (Fig. 17). t_{50} varied from 21 to 8 minutes, and DOC removal after 180 minutes of irradiation increased from 89 to 100% (experiments CLZ-L5 and CLZ-L7, respectively). These results suggested that the photo-Fenton degradation of clomazone in aqueous solution was less dependent of Fe(II) concentration when H_2O_2:C was at the maximum level. Moreover, the effect of [Fe(II)] on the initial pollutant degradation

rate seemed to be more important than on the long term COD removal.

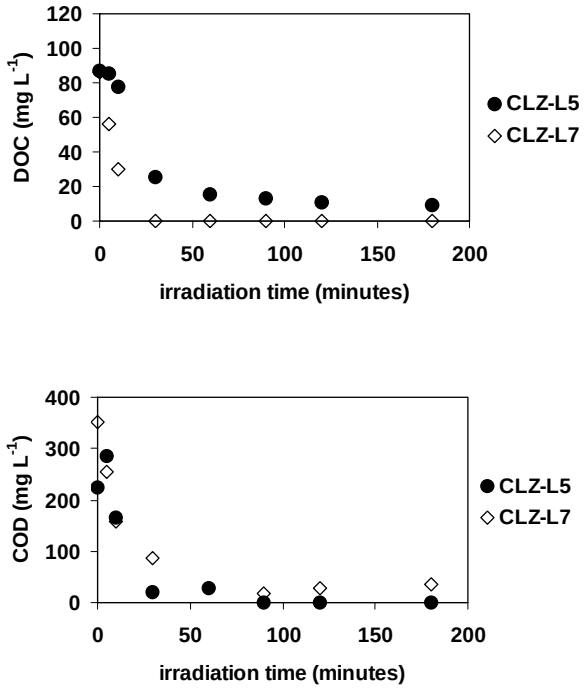

Figure 17 - Results of the photo-Fenton experiments carried out with clomazone at 30°C and H_2O_2:C=3.875, 125-W lamp. CLZ-L5 ([Fe(II)]=0.0001 mol L^{-1}); CLZ-L7 ([Fe(II)]=0.001 mol L^{-1}).

The central point of the Doehlert design (Fig. 12) was repeated at different conditions. Fig. 18 shows that clomazone was very stable under UV radiation, with a DOC removal less than 20% after 180 minutes of irradiation. When H_2O_2 was added, DOC values remained relatively constant up to ca. 60 minutes, followed by the oxidation of the pesticide with a DOC removal of 87%.

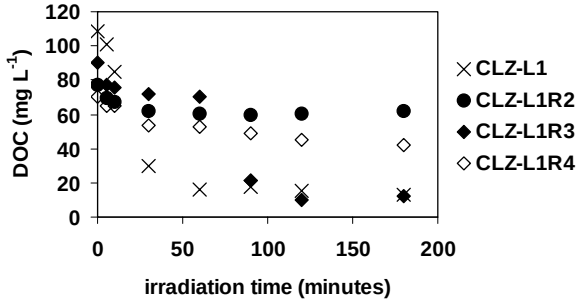

Figure 18 - Results of the experiments carried out at the central point of the Doehlert array at 30°C. CLZ-L1 (photo-Fenton; H_2O_2:C=2.75; [Fe(II)]=0.00055 mol L^{-1}; 125-W lamp); CLZ-L1R2 (UV; 125-W lamp); CLZ-L1R3 (H_2O_2/UV; H_2O_2:C=2.75; 125-W lamp); CLZ-L1R4 (Fenton; H_2O_2:C=2.75; [Fe(II)]=0.00055 mol L^{-1}).

The dark Fenton reaction enabled a faster initial degradation in comparison with the H_2O_2/UV process, but its long-term performance resulted in only 40% DOC removal. This was due to the cessation of $HO^{\bullet}$ radicals production after the complete conversion of Fe(II) to Fe(III) by reaction 1. The photochemically enhanced Fenton reaction, on the other hand, enabled to obtain residual DOC values (88% removal) after ca. 60 minutes.

The results of the Doehlert experimental design were analyzed using the software Statgraphics Plus 3.0. For the DOC percent removal (Y_1), the following quadratic response surface model was obtained:

$$Y_1 = 88 + 6.9X_1 + 5.8X_2 + 11X_1^2 + 12X_2^2 - 0.5X_1X_2 \quad (5)$$

For this model, R^2=0.89, the average of the residues (difference between experimental and calculated values of the response Y_1) is 2.17, and the average standard deviation of the residues is 1.54. No auto-correlation between the residues and the experimental and calculated values of the response, and the independent variables X_1 (H_2O_2:C) and X_2 ([Fe(II)]) was observed. Fig. 19 shows the response surface.

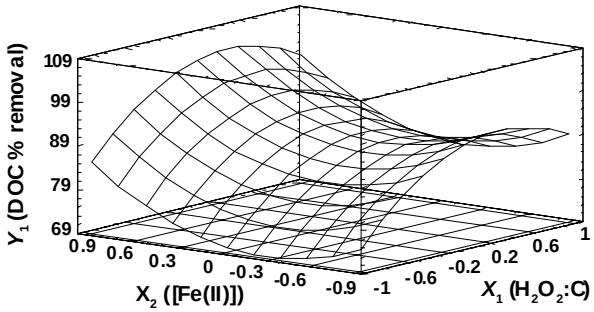

Figure 19 – Response surface for DOC removal in terms of normalized variables X_1 (H_2O_2:C) and X_2 ([Fe(II)]).

As discussed, the molar ratio H_2O_2:C has a remarkable effect on the DOC percent removal after 180 minutes of irradiation. At the two levels of [Fe(II)] considered, DOC removal increases with the increase in peroxide concentration, with a maximum at about H_2O_2:C=3.65. The subsequent decrease in DOC removal is probably due to the excess of peroxide. In this case $HO^{\bullet}$ radicals can be trapped by H_2O_2, leading to the formation of hydroperoxyl radicals ($HO_2^{\bullet}$) that are much less reactive than hydroxyl radicals.[2] Also, Fig. 19 shows that the DOC percent removal decreases with the decrease in [Fe(II)], particularly at H_2O_2:C=0.5 (X_1=-1). The model confirms the important conjoint effect exerted by Fe(II) and H_2O_2 on pesticide degradation.

In the case of t_{50} (Y_2), the quadratic surface response model is given by:

$$Y_2 = 18.8 - 25.7X_1 - 8.6X_2 + 28.6X_1^2 - 10.4X_2^2 + 11.4X_1X_2 \quad (6)$$

For this model, R^2=0.80, the average of the residues is 7.66, and the standard deviation of the residues is 5.08. No auto-correlation between the residues, the responses, and the independent variables was observed. The response surface (Fig. 20) shows that t_{50} notably decreases with the increase in the molar ratio H_2O_2:C, at both iron concentrations studied. For H_2O_2:C held at 0.5 (X_1=-1), t_{50} seems to decrease with the increase in Fe(II) concentration. The response surface suggests a region of minimum t_{50} about H_2O_2:C=3.65 and [Fe(II)]=0.0005 mol L^{-1}.

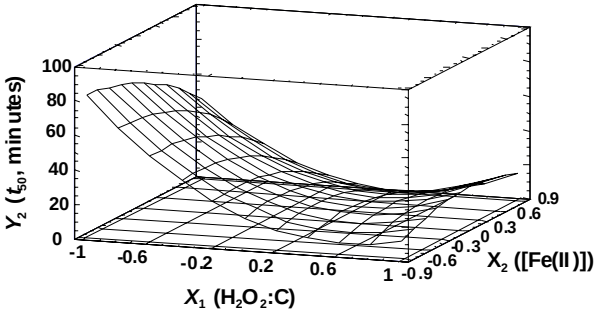

Figure 20 – Surface response for t_{50} (equation 6) in terms of normalized variables X_1 (H_2O_2:C) and X_2 ([Fe(II)]).

Some experiments of the Doehlert design (Fig. 12) were carried out in the parabolic trough solar reactor (PTR) at the same H_2O_2:C and [Fe(II)]. Solar irradiation conditions were in average similar to those illustrated in Fig. 3, corresponding to clear, sunny days with the sky free or almost free from moving clouds. Therefore, the accumulated direct energy input was comparable in most experiments during most of the time.

Fig. 21 compares DOC-time curves for experiments carried out at constant Fe(II) concentration and variable H_2O_2:C molar ratio. At [Fe(II)]=0.00055 mol L^{-1}, t_{50} varied from 67 to 12 minutes when H_2O_2:C varied from 0.5 to 5 (experiments CLZ-S3 and CLZ-S6, respectively); the corresponding DOC removals were similar after 180 minutes of solar irradiation, about 86%. At the maximum Fe(II) concentration, t_{50} varied from 23 to 16 minutes when H_2O_2:C varied from 1.625 to 3.875 (experiments CLZ-S2 and CLZ-S7, respectively). Total mineralization of clomazone was achieved in the first 90 minutes in experiment CLZ-S2; in experiment CLZ-S7, DOC removal after 180 minutes reached 92%. These results obtained in the parabolic trough solar reactor, parallel those depicted in Figs. 14 and 15 corresponding to lamp-irradiated systems. As expected, the values of t_{50} were generally higher under solar irradiation. For example, t_{50}=23 and 6 min (CLZ-S2 and CLZ-L2, respectively), and 12 and 8 min (CLZ-S6 and CLZ-L6, respectively). DOC percent removals after 180 minutes of irradiation were correspondingly similar.

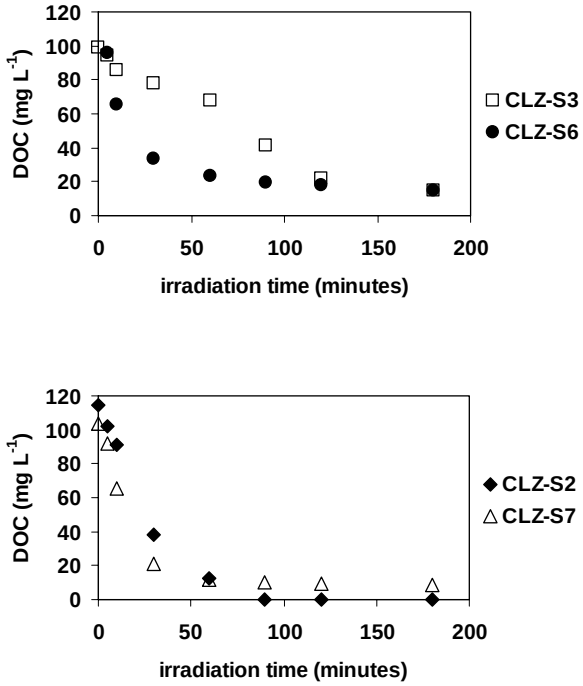

Figure 21 - Results of the photo-Fenton experiments carried out with clomazone in the solar PTR. CLZ-S2 (H_2O_2:C=1.625; [Fe(II)]=0.001 mol L^{-1}); CLZ-S3 (H_2O_2:C=0.5; [Fe(II)]=0.00055 mol L^{-1}); CLZ-S6 (H_2O_2:C=5; [Fe(II)]=0.00055 mol L^{-1}); CLZ-S7 (H_2O_2:C=3.875; [Fe(II)]=0.001 mol L^{-1}).

Fig. 22 compares the results of a solar experiment in which H_2O_2:C was held at 1.625 and [Fe(II)] was varied. The value of t_{50} was somewhat higher in experiment CLZ-S4 (31 minutes), as expected. DOC-time curves and DOC percent removals after 180m minutes were comparable, in contrast to the results obtained in the bench lamp reactor (Fig. 16). This behavior could be associate with the significant temperature increase observed under insolation in experiment CLZ-S4 (from 28 to 46°C), that could have quickened thermal oxidation reactions. pH values also underwent a higher decrease in experiment CLZ-S2 (from 3.04 to 2.19) in comparison with CLZ-S4 (3 to 2.42).

The comparison of experiment CLZ-S5 with experiments CLZ-S4 (at constant [Fe(II)]), and with CLZ-S7 (at constant H_2O_2:C) deserves careful analysis. At H_2O_2:C=3.875 (Fig. 23), the increase of Fe(II) concentration from 0.0001 to 0.001 mol L^{-1} led to a decrease in t_{50} from 54 to 16 minutes (experiments CLZ-S5 and CLZ-S7, respectively), while DOC percent removal varied from 79 to 92%.

These results are in agreement with those shown in Fig. 17, even though the values of t_{50} and DOC percent removal for experiment CLZ-S5 were notably different from those obtained in CLZ-L5 (21 minutes and 89%, respectively). Even considering the differences in initial DOC, Fig. 23 shows that the performance of experiment CLZ-S5 was unexpectedly poor in comparison with CLZ-S4, carried out at a lower H_2O_2:C ratio. This was due to the abrupt modification of sky conditions during the experiment CLZ-S5 (Fig. 24).

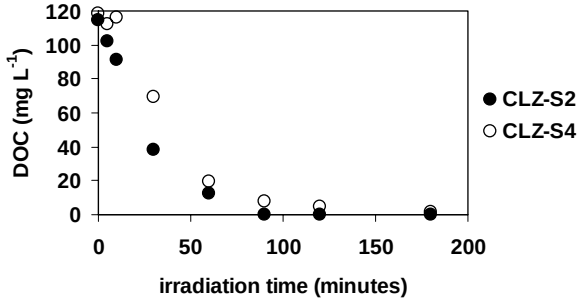

Figure 22 - Results of the photo-Fenton experiments carried out with clomazone in the solar PTR at H_2O_2:C=1.625. CLZ-S2 ([Fe(II)]=0.001 mol L^{-1}); CLZ-S4 ([Fe(II)]=0.0001 mol L^{-1}).

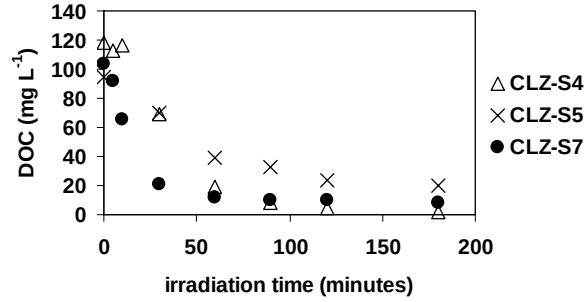

Figure 23 - Results of the photo-Fenton experiments carried out with clomazone in the solar PTR. CLZ-S4 (H_2O_2:C=1.625; [Fe(II)]=0.0001 mol L^{-1}); CLZ-S5 (H_2O_2:C=3.875; [Fe(II)]=0.0001 mol L^{-1}); CLZ-S7 (H_2O_2:C=3.875; [Fe(II)]=0.001 mol L^{-1}).

In solar photochemical reactors the incident radiation is not a manipulated variable, but may be treated as a measured disturbance in the process. Also, concentrating solar systems are not suited to capture diffuse sunlight under cloudy conditions as efficiently as they do for direct solar beams. The conditions mapped by the Doehlert matrix design may therefore provide a valuable guide to define operational strategies when atmospheric and weather conditions change in the course of the treatment process. For example, under insolation conditions like those shown in Fig. 3, lower levels of H_2O_2 and Fe(II) may be used, since solar light enhances the Fenton reaction, and comparable DOC removals are obtained. In the case of varying irradiance caused by the passage of clouds (Fig. 24), the values of H_2O_2:C and [Fe(II)] may be manipulated in such a way that the thermal Fenton reaction could compensate for the decrease in the photon input rate. This can also be possible after the middle afternoon when the irradiation naturally falls off. However, it should be emphasized that Fe(II) levels in disposed water are subject to environmental regulations, and together with H_2O_2, to economical restrictions.

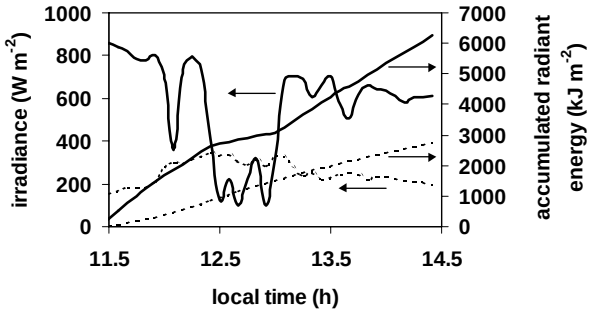

Figure 24 - Direct and diffuse (broken lines) radiation measurements (left ordinate axis) and corresponding accumulated radiant energy (right ordinate axis). Experiment CLZ-S5.

Conclusions

The experimental results presented in this work confirm the photo-Fenton reaction as a very effective process to oxidize agrochemicals of different chemical structures (fungicides, insecticides, herbicides etc.) in aqueous solutions. The process showed to be superior to other AOPs, at any Fe(II) and H_2O_2 concentrations, due to stronger light penetration and absorption up to 410 nm under homogeneous photocatalysis. In some cases, more than 90% of the DOC and COD could be removed after 180 minutes of irradiation, using 125 and 400-W mercury vapor lamps or under solar irradiation on clear sunny days. Pollutant removal was noticeably accelerated when [H_2O_2] or H_2O_2:C was increased at constant [Fe(II)]. This behavior makes the commercial use of solar-driven photo-Fenton processes environmentally attractive, lowering electrical energy costs. In this case, parabolic-trough solar reactors seem to an interesting technology. The increase in the BOD_5/COD ratio, in addition to the fast COD removal after short irradiation times suggest the use of the photo-Fenton reaction as a preliminary step prior to conventional biological treatment processes.

Acknowledgements

The authors would like to thank FAPESP and CNPq for financial support. Sincere thanks are also directed to Bayer CropScience, Clariant and to Prof. Dr. Gilberto Batista (LARP/ESALQ-USP), for pesticide samples, and to the Laboratory of Micrometeorology (Astronomical and Geophysical Institute, University of São Paulo) for solar radiation data.

Bibliography

(1) Burrows, H. D.; Canle, L. M.; Santaballa, J. A.; Steenken, S. (2002), Reaction pathways and mechanisms of photodegradation of pesticides. *J. Photochem. Photobiol. B - Biol.*, **67**, 71.

(2) Teixeira, A. C. S. C.; Guardani, R.; Nascimento, C. A. O. (2003), Solar photochemical degradation of aminosilicones contained in liquid effluents. Process studies and neural network modeling. *Ind. Eng. Chem. Res.*, **42**, 5751.

(3) Chiron, S.; Fernandez-Alba, A.; Rodriguez, A.; Garcia-Calvo, E. (1999), Pesticide chemical oxidation: state-of-the-art. *Water Res.*, **34**, 366.

(4) Will, I. B. S.; Moraes, J. E. F.; Teixeira, A. C .S. C.; Guardani, R.; Nascimento, C. A. O. (2004), Photodegradation of wastewater containing organic compounds in solar reactors. *Sep. Purif. Technol.*, **34**, 51.

(5) Teixeira, A. C. S. C.; Guardani, R. and Nascimento, C. A. O. (2004), Photo-Fenton remediation of wastewaters containing silicones: experimental study and neural network modeling. *Chem. Eng. Technol.*, **27**, 800.

(6) Nascimento, C. A. O.; Teixeira, A. C. S .C.; Guardani, R.; Quina, F. H.; Lopez-Gejo, J. (2004), Degradación Fotoquímica de Compuestos Orgánicos de Origen Industrial. In: Nudelman, N. (Ed.). Química Sustentable. Ediciones UNL - Universidad Nacional del Litoral, Santa Fé, Argentina, 206-220.

(7) Oliveros, E.; Legrini, O.; Hohl, M.; Müller, T.; Braun, A.M. (1997), Industrial wastewater treatment: large-scale development of a light-enhanced Fenton reaction. *Chem. Eng. Proc.,* **36**, 397.

(8) Bigda, R. (1995), Consider Fenton's chemistry for wastewater treatment. *Chem. Eng. Prog.*, (Dec.), 62.

(9) Bossmann, S. H.; Oliveros, E.; Göb, S.; Siegwart, S.; Dahlen, E. P.; Payawan, L.; Straub, M.; Wörner, M.; Braun, A. M. (1998), New evidence against hydroxyl radicals as reactive intermediates in the thermal and photochemically enhanced Fenton Reactions. *J. Phys. Chem. A*, **102**, 5542.

(10) Pozdnyakov. I. P.; Glebov, E. M.; Plyusnin, V. F.; Grivin, V. P.; Ivanov, Y. V.; Vorobyev, D. Y.; Bazhin, N. M. (2000), Mechanism of $Fe(OH)^{2+}$ (aq) photolysis in aqueous solution. *Pure Appl. Chem.*, **72**, 2187.

(11) Duffie, J. A.; Beckman, W. A. (1991), *Solar Engineering of Thermal Processes*, 2nd. Ed., Wiley, New York.

(12) Alfano, O. M.; Bahnemann, D.; Cassano, A. E.; Dillert, R.; Goslich, R. (2000), Photocatalysis in water environments using artificial and solar light. *Catal. Today*, **58**, 199.

(13) Acero, J. L.; Benitez, F. J.; Gonzalez, M.; Benitez, R. (2002), Kinetics of fenuron decomposition by single-chemical oxidants and combined systems. *Ind. Eng. Chem. Res.*, **41**, 4225.

(14) Standard Methods for the Examination of Water and Wastewater (1998), Clesceri, L. S.; Greenberg, A. E.; Eaton, A. D.; Franson, M. A. H. (Eds.). American Public Health Association, American Water Works Association and Water Environment Federation, Washington, DC.

(15) Vanhaecke, P.; Persoone, G.; Claus, C. (1980), Research on the development of a short-term standard toxicity test with *Artemia* nauplii. In: Persoone, G.; Sorgeloos, P.; Roels, O.; Jaspers, E. (Eds.). The Brine Shrimp *Artemia*. Morphology, Genetics, Radiobiology, Toxicology. Universo Press, Wetteren, Belgium, 263.

(16) Duménil, G.; Mattei, G.; Sergent, M.; Bertrand, J. C.; Laget, M.; Phan-Tan-Luu, R. (1988), Application of a Doehlert experimental design to the optimization of microbial degradation of crude oil in sea water by continuous culture. *Appl. Microbiol. Biotechnol*. **27**, 405.